Title: Temporal Change in Relationships Between Urban Structure and Surface Temperature

Authors: Justin D. Stewart[1,2], Peleg Kremer[2*],

[1]Department of Ecological Science, Vrije Universiteit Amsterdam, Amsterdam, The Netherlands
[2]Department of Geography and the Environment, Villanova University, Radnor, PA, USA

*Corresponding author
800 Lancaster Avenue, Villanova, PA 19085, USA
Department of Geography & the Environment
Villanova University
Phone: 610-519-3590
Email: peleg.kremer@villanova.edu

Author Contributions:

Conceptualization: PK, JDS
Formal data analysis: JDS, PK
Writing: JDS, PK

Keywords:

STURLA, Urban Structure, Surface Temperature, spatial-temporal change , New York City

Research highlights:

- The urban structure and surface temperature of New York City varied both between boroughs and within borough.
- Overall, the urban landscape become more homogenous over time.
- New York City grew vertically and on average became hotter in 2017 than it was 2008.
- Changes in urban structure influenced change in surface temperature, driven by water, lowrise buildings, and pavement.

Abstract:

Surface temperature influences human health directly and alters the biodiversity and productivity of the environment. While previous research has identified that the composition of urban landscapes influences the physical properties of the environment such as surface temperature, a generalizable and flexible framework is needed that can be used to compare cities across time and space. This study employs the Structure of Urban Landscapes (STURLA) classification combined with remote sensing of New York City's (NYC) surface temperature. These are then linked using machine learning and statistical modeling to identify how greenspace and the built environment influence urban surface temperature. It was observed that areas with urban units composed of largely the built environment hosted the hottest temperatures while those with vegetation and water were coolest. Likewise, this is reinforced by borough-level spatial differences in both urban structure and heat. Comparison of these relationships over the period between2008 and 2017 identified changes in surface temperature

that are likely due to the changes in prevalence in water, lowrise buildings, and pavement across the city. This research reinforces how human alteration of the environment changes ecosystem function and offers units of analysis that can be used for research and urban planning.

Introduction:

By 2030 it is projected that the majority of humanity will live in urban areas (DeSA, 2015) which are globally the fastest growing biome (Grimm et al., 2008). Matter and energy are consumed at greater quantities and frequencies in cities as compared to rural areas as a function of population demands (Fernández, 2007; Ratti et al., 2005). It is critical to identify patterns and processes of urban structure-ecosystem function relationships over temporal scales using a reproducible and scalable framework to meet and exceed the UN sustainable development goals (SDGs) by 2030 (Lu et al., 2015). The analysis of the urban landscape and ecosystem services provided over time can be used to inform management practices to encourage urban resilience (McPhearson et al., 2014; Walker et al., 2004) under global change scenarios.

Urban landscape topology is dependent on social, economic, technological, and environmental selective pressures that shape how a city is structured and will change over time. Neighborhoods and small towns emerge and coalesce into a larger urban units (Whitehand et al., 1996) across spatial scales (e.g. neighborhoods within a city or urbans centers connected in the Northeast United States megalopolis). Uneven resource distribution (e.g. food availability, work opportunities) further leads to heterogeneity in urban structure (Harris & Ullman, 1945). Likewise changes in structure over time are dependent on endogenous population growth and immigration-emigration tradeoffs as functions of the local economy (Black & Henderson, 1999).

Of particular interest within the urban landscape is surface temperature (ST), a physical property of the environment. In general, urban areas act as sinks for ST that are higher than surrounding rural areas (Howard, 2012) that can differ by city size. However, much variation in ST occur also with cities (Azhdari et al., 2018; Guo et al., 2020; Hamstead et al., 2016; Kremer et al., 2018). Variation of ST within the urban landscape is due to both seasonality and the physical makeup of the urban environment (such as pavement or vegetation that have different heat capacities) (Jayalakshmy & Philip, 2010; Oke, 1982). In a city, ST heterogeneity is amplified and modified by vertical structures. For example a highrise building casting a shadow and thus cooling an adjacent parcel of land (Kremer et al., 2018).

Numerous ecosystem aspects are subject to selective pressures of ST across functional (Morales et al., 2019) and taxonomic (Albright et al., 2011) based dimensions of biodiversity (García et al., 2018; Jenerette et al., 2007). Social and economic variables are also correlated with urban heat, including race (Huang & Cadenasso, 2016; Sanchez & Reames, 2019), income (Huang & Cadenasso, 2016; Wong et al., 2016), and education (Wong et al., 2016). Understanding how ST is structured across the urban landscape can help enhance sustainability, such as reducing residential water use (Guhathakurta & Gober, 2007; Zhou et al., 2017), as well as identify areas of spatial injustice within cities for vulnerable populations.

Preprints (www.preprints.org) | NOT PEER-REVIEWED | Posted: 10 May 2021 doi:10.20944/preprints202105.0199.v1

Within the context of these covariates, remote sensing of ST is often used as a proxy for the spatial distribution of multiple ecological variables and human wellbeing.

Likewise, landscape changes related to urbanization processes from vegetation to built environment have been linked to urban ST (Oke, 1995). However, less is known about the changes within an established urban environment over time. STructure of URban LAndscape (STURLA) studies have demonstrated that urban structure in New York City (NYC), Berlin, and Philadelphia can be explained by a discrete number of heterogeneously distributed three-dimensional 120m^2 cells composed of differing landscape elements (e.g. trees or highrise buildings) (Hamstead et al., 2016). Previously STURLA has been used to investigate ST (Hamstead et al., 2016; Kremer et al., 2018; Larondelle et al., 2014; Mitz et al., 2021), phylogenetic structure of the atmospheric microbiome (Stewart et al., 2021) and particulate air pollution (Cummings et al., 2021). STURLA captures urban spatial patterns that historically have been difficult to quantify due to the high density and the patchy nature of spatial patterns within a city.

Likewise, STURLA is a classification model that differs from the commonly used land use land cover (LULC) based model in that it incorporates more information (e.g. compositional sums of landscape elements) withing a single unit. This allows for a more flexible and generalizable framework that can take into account interactions between these elements such, as a tree shading pavement. Such Interactions that may influence variables (e.g. ST) are unaccounted for in LULC models which use individual pixels that represent a single quantity such as pavement or grass. STURLA offers a simple way to understand units of urban structure that can be applied to planning efforts for sustainable development across cities and over years. In this paper we apply STURLA to a spatial-temporal process for the first time. We explore the changes in surface temperature over time by linking together changes in urban structure in New York City. This is extended by using the STURLA classification system combined with machine learning to model ST in 2008, 2017, and the change between the years.

Material and Methods:

Site Description:

New York City (NYC) is largest city in the United States of America with a 2019 estimated population of over an estimated 8,336800 residents (United States Census Burough, 2016) ~740 km^2. Located on the eastern part of the continental United States, NYC is split into five boroughs (Brooklyn, The Bronx, Queens, Staten Island, and Manhattan) of varying size, populations, and socio-economic class.

Urban Structure:

STURLA datasets were constructed using a 120 m grid aligned to the ST datasets for each 2008 and 2017. Following (Hamstead et al., 2016) a zonal statistics tabulate area operation computed the area of a combined land cover and building height dataset within each cell. Building height was access from the NYC MapPluto database (NYC Department of City Planning, 2021) for each year. Within pixel elements are then summed to create a final STURLA class. For example, if any percentage greater than 0.0% of trees, grass, pavement, and low-rise buildings is present, that pixel will be coded with *tgpl*. Finally, we generated and assigned a

 doi:10.20944/preprints202105.0199.v1

STURLA class variable for each grid cell. Examples of coded STURLA pixels can be found in Figure 1A. Maps of example parks (Supplemental Figure 1) and boroughs (Supplemental Figure 2) can be found in supplemental for reference.

ST Acquisition and Processing:

ST data were accessed from the United States Geological Survey (USGS) Earth Explorer using Landsat 7 Analysis Ready Data (ARD). ARD data are corrected, pre-processed and converted to ST (in degrees Celsius) by the USGS. After downloading, mean zonal statistics were calculated per STURLA pixel for each raster. All available ST rasters for the defined time period that contained less than 30% cloud cover over the NYC boundaries were used. The time period was chosen as between June 21st and September 22nd for each year as it would allow us to look at both the mean across days and the variance between them (Hamstead et al., 2016; Mitz et al., 2021). Likewise these provide a wide representation of summer temperatures to validate that STURLA identifies patterns between urban structure and ecosystem function and thus be used in future urban planning practices. To validate that ST trends observed between the two years were not heavily subject to climactic/weather anomalies a permutation Pearson correlation model was constructed (see Supplemental Figure 3). This model revealed significant and strong relationships between the two years and suggests that direct comparisons of the two years is valid.

Data Analysis and Visualization:

All datasets were projected to NAD 1983 State Plane New York Long Island FIPS 3104 Meters. Quantile classification is used in all maps as this allows for comparison of the distribution of data across the years. Statistical analysis was done in R. 4.0.1. Similarity of ST hosted in STURLA classes was determined using hierarchical clustering with Bray-Curtis dissimilarity. This method was chosen as it is qualitative and allows for compositional comparison between ST by STURLA class (Figure 2C-D). ST values were visualized with a heatmap using scaled and centered data to allow comparability between the years. Landscape heterogeneity was calculated as the sum of landscape elements within a pixel (comprising 1 STURLA class) for all years and change was calculated as the heterogeneity in a pixel of 2008 minus that of 2017. For example, STURLA class *bpl* has a heterogeneity value of 3. Change in surface temperature likewise was calculated as 2008 ST minus 2017 ST.

Supervised machine learning, Random Forest Regression (RFR), models using the *caret* package (Kuhn, 2008) were used to estimate the strength of the relationship between STURLA classes and mean ST per class. This model was chosen because it was previously shown to better handle non-parametric spatial data when compared to linear models (W. Chen et al., 2017; Oliveira et al., 2012). Classes with less than 100 pixels were removed as these more infrequent classes likely have less of a role in overall patterns of surface temperature. Models were built as: Mean ST per STURLA class ~ Trees % + Grass % + Bare Soil % + Water % + Pavement % + Low-rise % + Midrise % + Highrise %. For this, data was partitioned into 60% training and 40% validation sets that underwent 10-fold repeated cross validation. Trained models were then used to predict mean ST when given a STURLA class which were then projected to each pixel in the STURLA grid. Root Mean Standard Error (RMSE) was used to

Preprints (www.preprints.org) | NOT PEER-REVIEWED | Posted: 10 May 2021 doi:10.20944/preprints202105.0199.v1

quantify average model error. Variable importance was measured using the *varImp* function and then scaled from 0-100 where values closer to 100 are more important for model accuracy and error reduction. The same process was applied to identify the mean change in ST per STURLA class and the mean change in landscape component percentages. To better represent model results the top and bottom 1.0% of model predictions and subsequent errors were excluded from mapping.

To account for spatial and temporal autocorrelation, permutational methods are used to estimate a distribution from which to generate a p-value. This means that the distribution is not structured through a spatial process as the randomization breaks this down by resampling the parameter values. Permutational Spearman correlations using *wPerm* (Weiss, n.d.) were used to identify relationships between individual STURLA landscape elements (e.g. *h*) with ST for each year as well as change in ST. Permutation also allows for comparison of ST as the values for each year are drawn from a similar urban landscape and thus similar underlying distribution. Differences in changes in STURLA heterogeneity and ST by borough was tested using permutational T-Tests using package *RVAideMemoire* (Hervé, 2020). Data and code for these analyses can be found at https://github.com/thecrobe/STURLA_NYCChange.

Results:

NYC STURLA Structure

The ten most frequent STURLA classes (Figure 1A) explained 60.84% and 80.01% of NYC's structure in 2008 and 2017 respectively (Figure 1D-E). For 2008 and 2017 only 15 STURLA classes contained exclusively the natural environment (classes composed of combinations of *t, g, b, w*) that cover a mean between the years of 5.69% of NYC's landscape. In 2008 the most common STURLA class per borough were *tgpl* in Brooklyn (9.85%), Staten Island (26.32%), and Queens (24.36%). Class *tgp* dominated The Bronx (13.04%) and *tph* in Manhattan (19.94%).

In 2017 class *tgpl* was still the most frequent (and became more abundant) in Staten Island (36.46%) and Queens (34.37%). Relatively large changes in urban structure occurred for Brooklyn, The Bronx, and Manhattan. Class *tgplmh* dominated Brooklyn (34.79%) and demonstrated gains and transitions from the 2008 most abundant class, *tgpl*. Class *tgph* (21.58 %) replaces *tph* as the most common in Manhattan. The Bronx grew vertically with class *tgplmh* becoming most frequent (20.51%). Spatial distribution of STURLA classes was heterogenous; however, specific classes clustered throughout the city (e.g. *tgp* in Highland Park and Floyd Bennet Field in Brooklyn). Likewise, classes with *h* were largely found in Manhattan (*tgph*) and Brooklyn (*tgplmh)*.

Preprints (www.preprints.org) | NOT PEER-REVIEWED | Posted: 10 May 2021 doi:10.20944/preprints202105.0199.v1

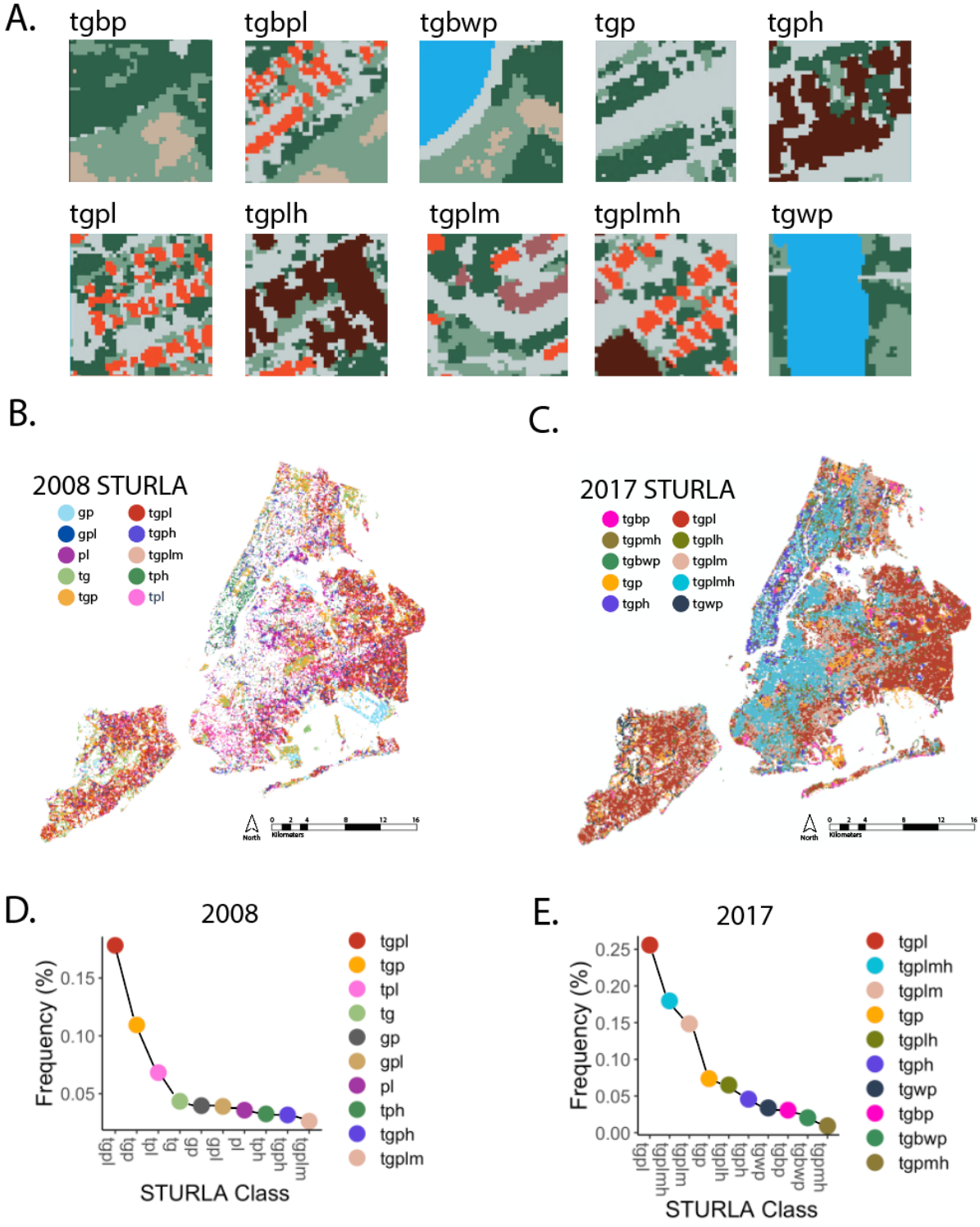

Figure 1: A. Examples of the most frequent STURLA classes in NYC 2008 colored by landscape component (trees: dark green, grass: light green, bare soil: beige, pavement: grey, bright red:

 doi:10.20944/preprints202105.0199.v1

lowrise buildings, medium red: midrise buildings, dark red: highrise buildings). Map of the spatial distribution of STURLA classes for NYC 2008. Map of the spatial distribution of STURLA classes for NYC 2017. D. Ranked frequency plot of STURLA classes in NYC 2008. E. Ranked frequency plot of STURLA classes in NYC 2017.

NYC Surface Temperature

NYC 2008 ST ranged from 21.30°C to 46.57°C across the urban landscape with a mean of 32.24°C. Each borough hosted unique ST values that significantly differed from each other (all $p<0.002$) with the exception of The Bronx and Staten Island ($p=0.48$) and Staten Island with Queens ($p=0.992$). The hottest borough on average was Queens (34.19°C) followed by Brooklyn (33.83°C), The Bronx (32.62°C), Staten Island (32.59°C), and Manhattan (32.23°C). In 2017, NYC had a narrower range in ST than 2008 with from 18.23°C to 43.87°C with a higher mean of 32.77°C. For 2017 the hottest borough on average was still Queens (33.46°C) followed by Brooklyn (32.75°C), The Bronx (32.51°C), Manhattan (32.19°C), and Staten Island (31.97°C). Similar to 2008, in 2017 each borough hosted unique ST values that significantly differed ($p<0.002$) from each other still excluding The Bronx and Staten Island ($p=0.48$). In contrast, Manhattan and Staten Island differed ($p=0.778$) in ST signatures in 2008.

Distinct patterns of ST within the city emerged across the years. Greenspaces such as Central Park in Manhattan hosted lower surface temperatures than the surrounding STURLA classes that have greater proportions of the built environment (Figure 1B-C, Figure 2A-B). Similar patterns can be found in other parks/greenspaces across the city (e.g. Pelham Bay Park, Staten Island Greenbelt, Prospect Park in Brooklyn). ST was highest in STURLA classes where the built environment dominated (Figure 2C-D, e.g. *gpl, tpl, p, pl, pm*). Likewise, ST was lowest in STURLA classes where there was no built environment (Figure 2C-D, e.g. *tgbw, tgw, gbw, gw, w*). These patterns are intensified in 2017 as the built environment (classes with *p, l, m, h*) clusters more than in 2008 and host the highest ST across the landscape. Conversely, STURLA classes with water cluster more readily and host the lowest ST.

Preprints (www.preprints.org) | NOT PEER-REVIEWED | Posted: 10 May 2021 doi:10.20944/preprints202105.0199.v1

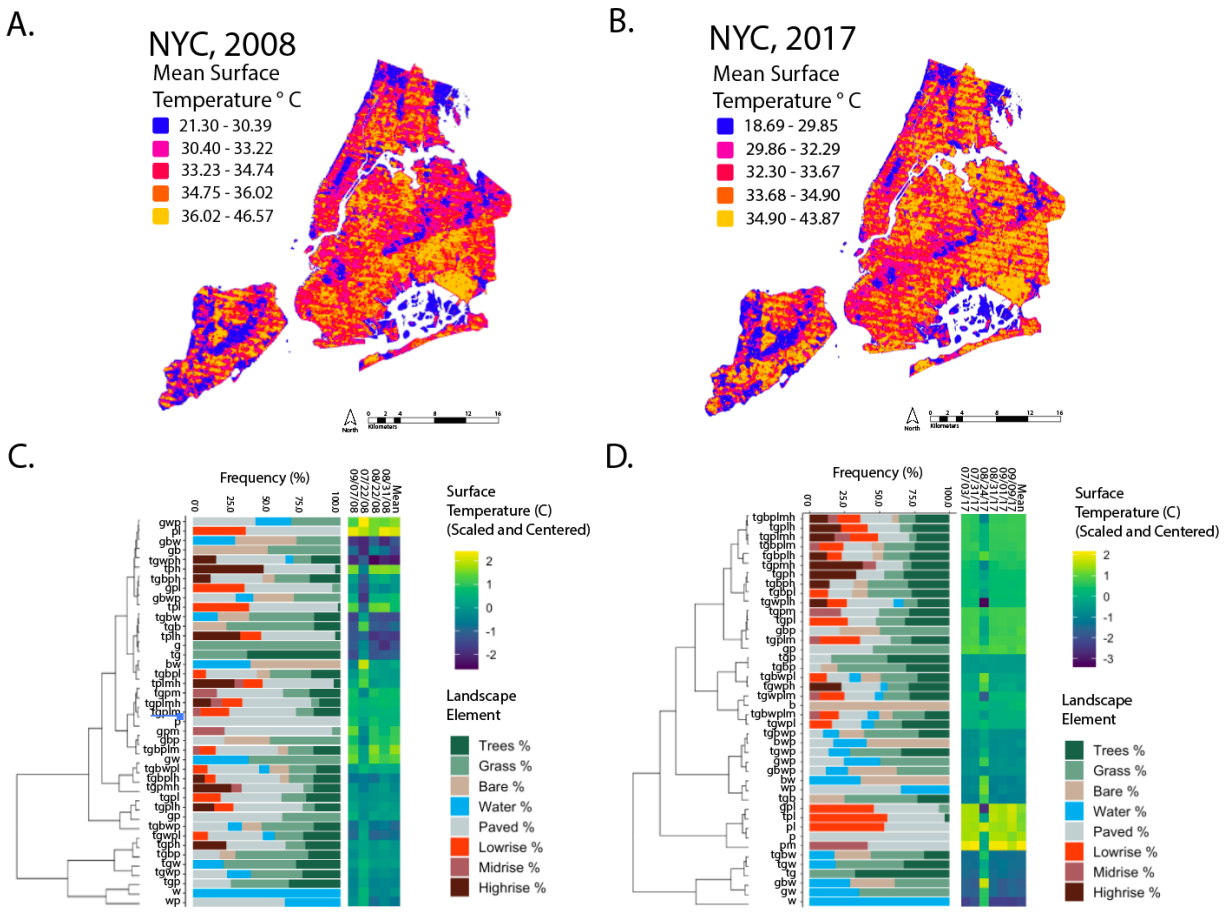

Figure 2: A. Map of ST in NYC 2008 where colors closer to blue indicate lower values and closer to red being higher. B. Map of ST in NYC 2017 where colors closer to blue indicate lower values and closer to red being higher. C. 2008 Hierarchically clustered heatmap of ST values showing the ST for each day an a mean value as the final column on the right. Between heatmap and dendrogram a stacked barplot of the mean internal landscape compositions for each STURLA class is shown. D. 2017 Hierarchically clustered heatmap of ST values showing the ST for each day an a mean value as the final column on the right. Between heatmap and dendrogram a stacked barplot of the mean internal landscape compositions for each STURLA class is shown. The reader is encouraged to download and zoom into this figure if interested in specific STURLA classes.

Change in Urban Structure and Surface Temperature

NYC's urban structure became more homogenous as the number of STURLA classes decreased from 139 classes in 2008 to 118 classes in 2017; however individual STURLA pixels generally became more heterogenous and gained landscape elements (Figure 3B, e.g. *t* or *p*). Changes in STURLA classes were not uniform as some STURLA pixels greatly changed, for example the addition of a green roof in Figure 3A, while others remained relatively the same. An average of +1.344 landscape elements were gained (Figure 3B, e.g. a tpl pixel 2008 gaining *g* and becoming *tgpl*). On average, Manhattan (+1.768) gained the most internal landscape elements followed by Brooklyn (+1.626), The Bronx (+1.544), Queens (+1.123), and Staten

Preprints (www.preprints.org) | NOT PEER-REVIEWED | Posted: 10 May 2021 doi:10.20944/preprints202105.0199.v1

Island (+1.097). Each borough gained STURLA class elements differently (all $p < 0.002$). STURLA classes composed of a mixture of the built and natural environment (e.g. Midtown Manhattan and Brooklyn) experienced greater gains in the number of STURLA elements across the city as compared to greenspaces (e.g. parks) which became more homogenous despite additions of different landscape elements.

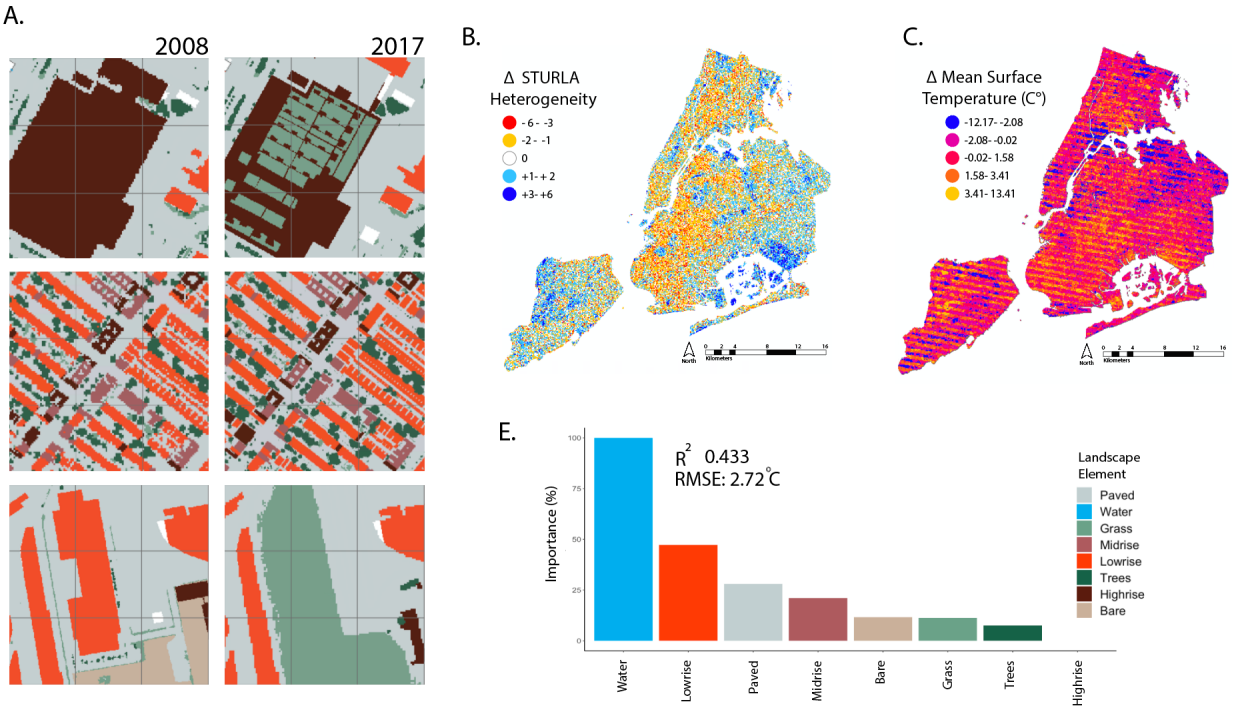

Figure 3: A. Example of STURLA pixels that underwent different degrees of change in structure. B. Map of change in STURLA class heterogeneity. C. Map of change in mean surface temperature. D. Random Forest regression variable importance for Δ ST as a function of Δ in landscape element percentages.

Across NYC as a whole, ST per pixel increased from 2008 to 2017 by a mean of +0.47°C (Figure 3C). Changes in ST also varied by borough ($p>0.002$) with the exception of The Bronx with Manhattan ($p=0.454$), Manhattan with Queens ($p=0.084$), and Queens with Staten Island ($p=0.966$). Decreases in ST were largely found in Brooklyn, South Queens, Central Staten Island, and the South Bronx. ST increased in North Queens and Manhattan, and South Staten Island. ST change for the most ten frequent classes were *tgpl* (-3.57°C), *tgplmh* (-2.88°C), *tgplm* (-3.49 °C), *tgp* (+0.212°C), *tgplh* (-3.30°C), *tgph* (-2.29°C), *tgwp* (+1.24°C), *tgbp* (0.24 °C), *tgbwp* (+0.92 °C), and *tgpmh* (-2.76 °C).

Change in ST modeled as a function of changes in internal STURLA components (e.g. mean percentage of *t* decreasing 0.03% in class *tgpl*) revealed a moderate relationship (Figure 3E, R^2= 0.433, RMSE: 2.72°C). This association was driven by changes in water, lowrise buildings, and pavement (all variable importance > 25%). Likewise, modeling at the STURLA class level outperforms correlations between individual STURLA elements (e.g. change in ST ~ change in percentage *t*) (Table 1). Univariate correlations between change in ST demonstrated significant

Preprints (www.preprints.org) | NOT PEER-REVIEWED | Posted: 10 May 2021 doi:10.20944/preprints202105.0199.v1

(p>0.05) relationships with bare soil, water, lowrise, and midrise within STURLA class percentages (Table 1). ST decreased with increasing amounts of bare soil and water while the opposite relationships were observed for the built environment. A permutational model testing the relationship between ST in 2008 to ST in 2017 per STURLA pixel revealed a strong positive correlation (Supplemental Figure 1, R^2:0.815, $p < 0.0001$) and suggests that the majority of variation in ST is due to urban structure; however, climactic trends may also influence this study's results but to a relatively small degree. Likewise, moderate to strong significant positive correlations were found between ST for each year when separated by STURLA class; however the strength of the relationship varied by class (Figure 4).

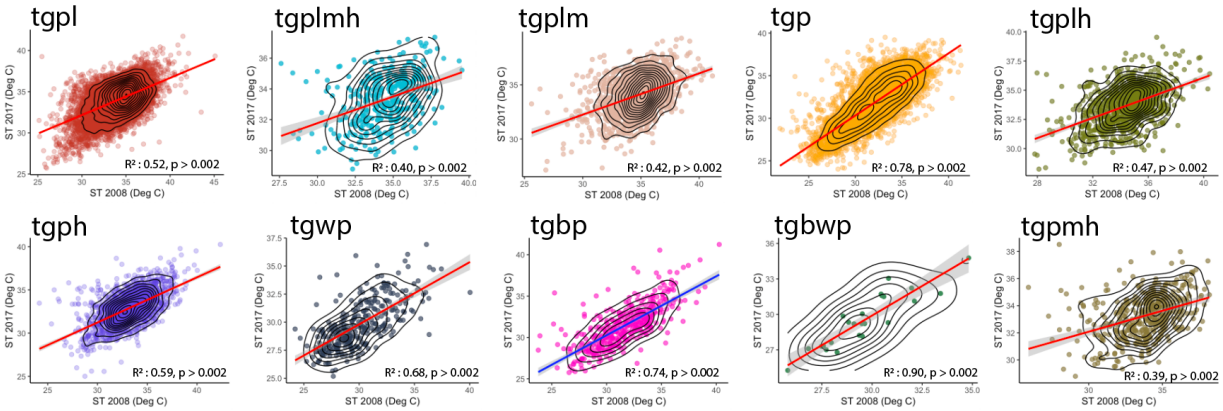

Figure 4. Multipanel of permutational spearman correlation models for between ST in 2008 and 2017 for STURLA pixels that did not change in heterogeneity (e.g. change from tgpl to tpglmh). The top ten most frequent classes for 2017 are shown with density plots of their joint marginal distribution and lines to show the linear fit. Each plot is colored by STURLA class as see in the ranked abundance plots and maps.

Table 1: STURLA landscape element magnitude and direction estimation. This table contains the correlation coefficients (Rho) from permutational spearman correlations. Bold values indicate p < 0.05 for the correlation model. All other correlations were insignificant

Landscape Element	**ST 2008 Rho**	**ST 2017 Rho**	**Δ ST Rho**
Trees (t)	**-0.3029518**	**-0.3783883**	-0.0748541
Grass (g)	-0.2329279	**-0.5187178**	-0.048151
Bare soil (b)	-0.1244753	**-0.2990706**	**-0.2206849**
Water (w)	-0.0900591	**-0.5546377**	**-0.2483849**
Paved (p)	**0.3435931**	**0.6463642**	-0.0683169
Lowrise (l)	0.1898042	**0.5166262**	**0.3812218**
Midrise (m)	0.3262976	**0.3272964**	**0.2108852**
Highrise (h)	-0.1264511	**0.3135041**	0.02940633

Preprints (www.preprints.org) | NOT PEER-REVIEWED | Posted: 10 May 2021 doi:10.20944/preprints202105.0199.v1

ST Prediction by STURLA Class

STURLA classes were able to explain and predict ST across NYC for both 2008 (R^2:0.788, RMSE:0.34°C) and 2017 (R^2:0.788, RMSE: 1.90°C) better than any individual within class landscape element (Table 1). Despite strong correlations between urban structure and ST, the relative role of STURLA internal class elements differed. 2008 models relied on paved, trees, highrise, grass, and bare soil to predict ST (Figure 5A, all variable importance > 25%). In contrast 2017 ST was largely predicted by the presence and distribution of STURLA classes with pavement and water (Figure 5D, all variable importance > 25%). Both models predicted higher ST in classes hosting the built environment (e.g. *tgplm*, Figures 5B,5E) and lower temperatures in those that are partially vegetated (e.g. *tgp, tg*). Predicted values were greater in 2017 than 2008. Models overpredicted ST in areas with greenspace (e.g. parks) and STURLA classes dominated by bare soil for both years (Figures 5C,5F). In contrast they underpredicted where classes *tgpl* and *tgplmh* dominated.

Univariate correlations estimate the direction of each variable on STURLA class ST as it cannot be inferred from Random Forests. In 2008, percentage paved had significant positive relationships with ST. For 2017 all within class elements had significant relationships (p>0.05) with ST. As percentages of trees, grass, bare soil, and water increase, mean ST per STURLA class decreased. The opposite relationship was found where ST increased as the percentages of the built environment (paved, lowrise, midrise, and highrise) also increased.

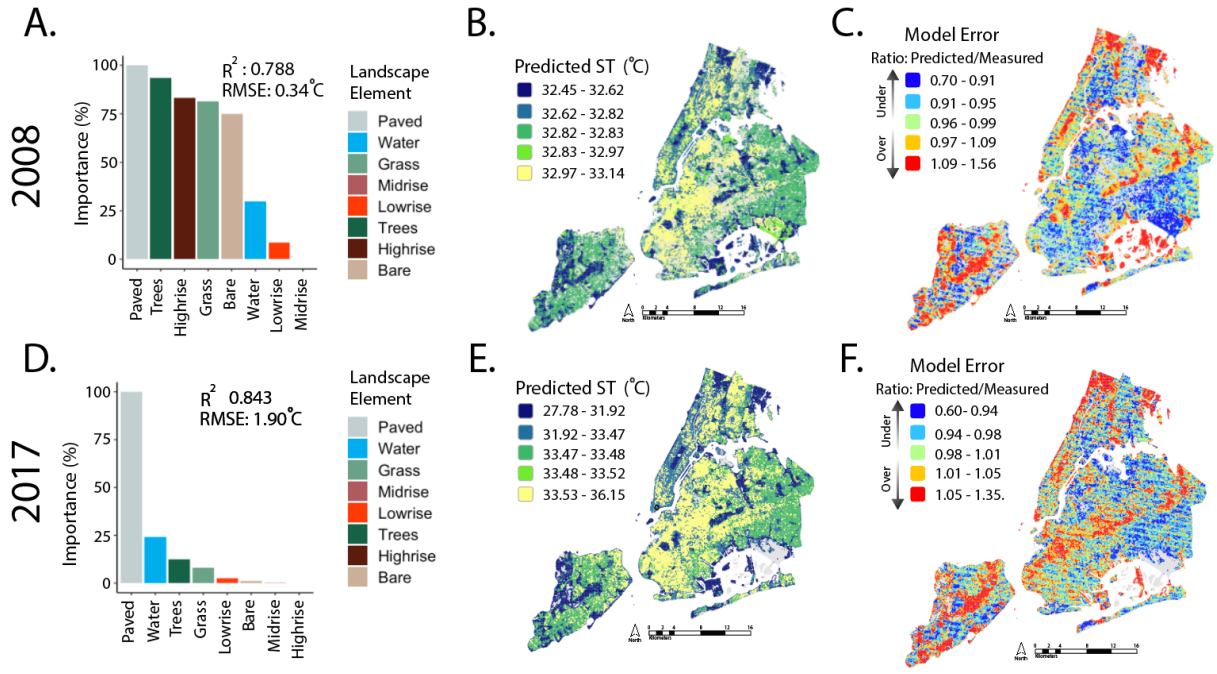

Figure 5. A. 2008 Random Forest regression variable importance for ST prediction with coefficient and error at the top left. B. 2008 Map of predicted ST per STURLA class where darker colors indicate lower ST and lighter colors being higher ST. C. 2008 Model error from Random Forest regression shown as a ratio of predicted/measured ST. D. 2017 Random Forest regression variable importance for ST prediction with coefficient and error at the top left. B. 2017 Map of predicted ST per STURLA class where darker colors indicate lower ST and lighter

Preprints (www.preprints.org) | NOT PEER-REVIEWED | Posted: 10 May 2021 doi:10.20944/preprints202105.0199.v1

colors being higher ST. C. 2017 Model error from Random Forest regression shown as a ratio of predicted/measured ST.

Discussion:

NYC Urban Structure

The urban landscape for both years was unsurprisingly dominated by STURLA classes with the built environment with the exception of established parks and greenspaces. Likewise, the city as a whole, grew vertically as *l*, *m*, and *h* STURLA elements were commonly added. Brooklyn experienced the greatest change in the vertical dimensions as classes *tgpl* and *tgp* transitioned to *tgplmh*. With the growth in these vertical landscape elements, a relative shift in the internal landscape proportions of the classes in Brooklyn and The Bronx occurs as a function of STURLA's compositional (sum to 100%) nature. The additions of landscape elements *m* and *h* to these boroughs may be a function of a continued pattern of gentrification in NYC (Hackworth & Smith, 2001; Lees, 2003). Furthermore, the rapid pace of urban change through a gentrifying lens differs from historical patterns in that the landscape is being changed not by individuals renovating single homes or businesses but by large scale developers and financiers. Wealthy corporations are able to finance larger scale urban development (e.g. construction of a new highrise building and thus adding in an *h* element to a STURLA class) more than the individual's purchasing power allows (Lees, 2000).

These studies taken together with our results suggests continued urban development in the form of gentrification may be one of the many driving forces behind the homogenization of the urban landscape over time as the diversity of STURLA classes decreases in exchange for units of new urban development (such as *lmh*). A prominent example of this modification can be found along the Highline park constructed on an old, elevated railway track along the Meatpacking District and Chelsea in Manhattan. The construction of the Highline coupled with the growing desirability of living in these areas as new global epicenters of the art world (Molnár, 2017) and proximity to the Hudson Yards project led to changes in the urban landscape. The approximate 20,000 of residential units with a wide range in socio-economic class of renters and owners were and are being replaced by retail and (Haase et al., 2017; Hudson Yards Development Corporation; Wolch et al., 2014) housing that shifts both the social structure (Patrick, 2014) of the area but the physical ST of the city as well. Other examples of park construction that has led to gentrification and subsequent change in urban topology and ecosystem function (ST) include Hunter's Point South park in Queens and Domino park in Williamsburg, Brooklyn.

Likewise, changes in urban structure also arise from natural disasters and poor prior planning for urban structural resilience. This becomes apparent when the effects of 2012 Hurricane Sandy on Lower Manhattan and Queens/The Rockaways are compared. Lower Manhattan with access to financial capital was able to respond to and recover from the hurricane much more readily than other areas of the city that were affected (New York Downtown Alliance, 2013). This allowed highrise buildings to be rapidly renovated and new development to be introduced into the urban landscape. In comparison the socially diverse and low-mid income Queens and Rockaways urban structures that were destroyed by the hurricane, recovered (if at all) at a much slower pace. Likewise, much of the housing and educational

 doi:10.20944/preprints202105.0199.v1

infrastructure in these locations was federally funded and had considerably less financial resources to rebuild compared to the wealth in Manhattan. Thus, the differences in rates of rebuilding and redevelopment have likely influenced urban ST patterns that continue to persist and are apparent in our results .

3D Urban Structure Influences Surface Temperature

STURLA captured the urban structure-heat relationship as demonstrated by STURLA classes hosting unique ST values and robust correlations with relatively low error across the urban landscape. Furthermore, STURLA models displayed better associations and more robust predictions than other 2-dimensional models of urban structure (Connors et al., 2013). This is due to each STURLA class being able to contain differing percentages of each landscape element, thus offering a more realistic representation of urban structure. Despite this, limitations do exist, for example, two pixel of STURLA class *gwp* may contain vastly differing percentages of grass, water, and pavement. These compositional variations may be sources of error in models as a function of uncertainty propagation. Likewise, the within class variation and neighborhood effects of nearby pixels of same or different STURLA classes may be influencing local ST signatures as demonstrated in Berlin (Kremer et al., 2018). This could be seen where a pixel coded as STURLA class *p* neighbors a *tgph* pixel that may cast a shadow on the *p* pixel and thus cool the first pixel's relative ST compared to other *p* pixels across the city.

Our findings that STURLA classes composed largely of the built environment host higher ST values complement studies in cities of varying sizes across the globe with different climates and biomes: Beijing (Kuang et al., 2014), Berlin (Kottmeier et al., 2007; Kremer et al., 2018), Lagos (OS & AA, 2016), Kunming (X. Chen & Zhang, 2017), Melbourne (Jamei et al., 2019), New York City (Hamstead et al., 2016; Susca et al., 2011), Phoenix (Buyantuyev & Wu, 2010; Connors et al., 2013), Tehran (Bokaie et al., 2016), and Vancouver (Voogt & Oke, 1998). In contrast, pixels and STURLA classes with greater proportions of greenspace (containing *t* and or *g*) hosted lower ST signatures. This further highlights the importance of incorporating greenspace heterogeneously in urban areas. Currently in NYC the majority of planned greenspace is clustered in parks and has subsequent social implications such as changing desirability (more greenspace being more desirable) and then subsequent housing prices.

This clustering also creates areas of low ST that have to be sought out by individuals (lower income populations) to obtain their benefits given those with greater financial means often live closer to parks (Shanahan et al., 2014). Addition of greenspace in cities may benefit from a large number of small vegetative units more evenly dispersed throughout the landscape than construction of new relatively larger parks. A potential example of this would be rewilding (Danford et al., 2018) vacant lots as urban hotspots of vegetative biodiversity. As long as these areas become established patches of urban nature and not transient, they would provide numerous ecosystem services including reduced ST, access to healthy microbial populations (Kremer et al., 2013; Mills et al., 2017; Rook, 2013), and increase human-nature interactions that are at risk in cities (Cox et al., 2017; Keniger et al., 2013; Soga et al., 2015). The relatively small units of land comprising a STURLA pixel and generalizable nature of STURLA could be used to plan the incorporation specific urban units such as *tgbw or gbw* that host lower ST values in other cities.

Preprints (www.preprints.org) | NOT PEER-REVIEWED | Posted: 10 May 2021 doi:10.20944/preprints202105.0199.v1

Conclusion:

In this paper we used remote sensing of urban heat with the STURLA method that were linked together by machine learning and statistical modeling to identify the urban spatial-temporal structure-surface temperature relationship in NYC over a decade. Understanding these dynamics is crucial to future sustainable and egalitarian urban planning given how urban surface temperature influences human wellbeing and urban biodiversity. We conclude that NYC as a whole is becoming more homogenous while adding in more vertical elements of the built environment and is warming on average. Likewise, these changes are linked to specific three-dimensional urban units where heat signatures are lowest in those dominated by vegetation and water and highest in those where pavement, lowrise, and midrise buildings are present and prevalent. This study reinforces that STURLA is a computationally inexpensive model and aids in understanding ST effects and offers context for sustainable development and urban planning. Limitations of this study include an analysis of only two timepoints and STURLA being agnostic to the physical composition of building materials and the influence of species and functional traits in the vegetative elements of a STURLA class. Future studies should incorporate other measures of urban ecosystems such as plant biodiversity.

Funding: This project is funded by NSF award # 1832407.

Supplemental:

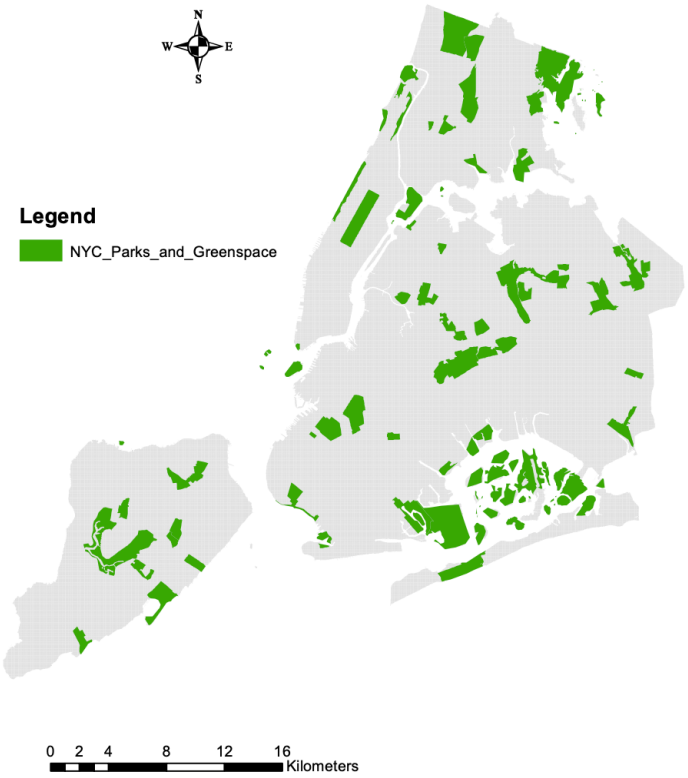

Supplemental Figure 1: Map of NYC parks and greenspace

Preprints (www.preprints.org) | NOT PEER-REVIEWED | Posted: 10 May 2021 doi:10.20944/preprints202105.0199.v1

456

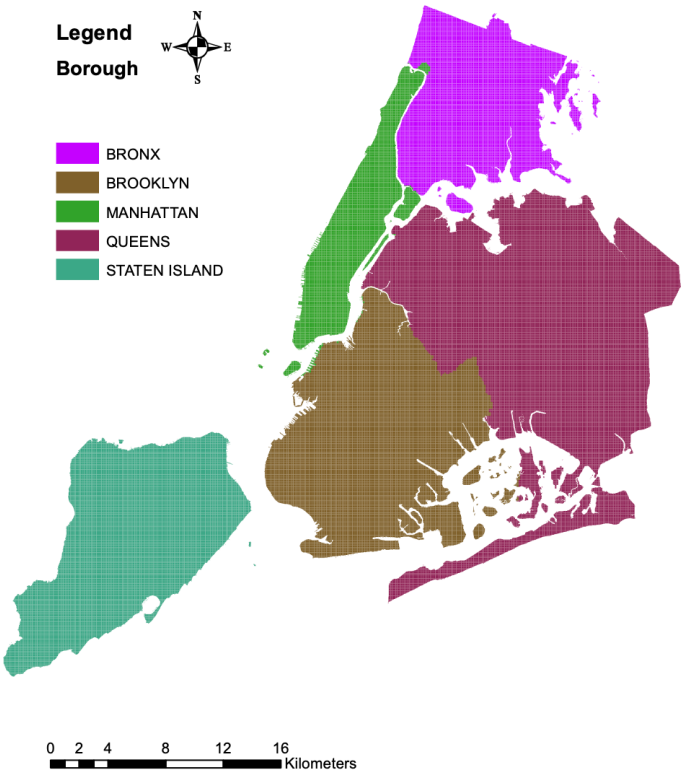

457
458 Supplemental Figure 2: Map of NYC boroughs.
459
460

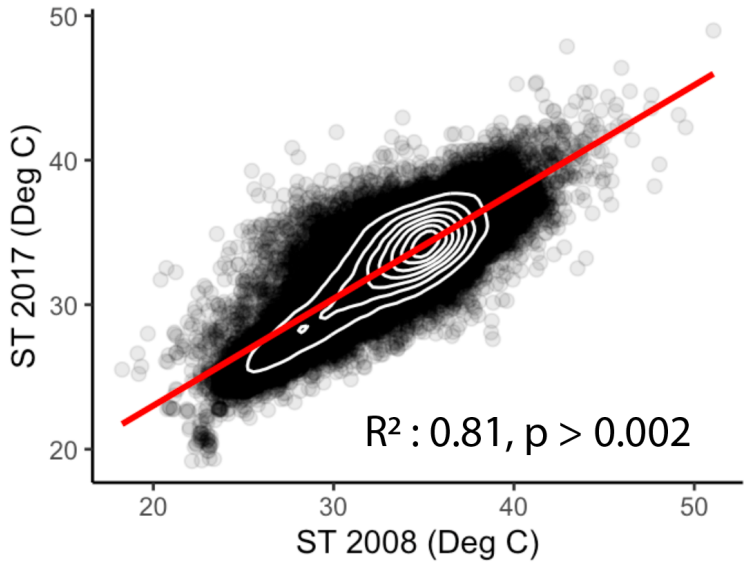

461
462 Supplemental Figure 3: Permutation spearman correlation between ST in 2008 and in 2017. The
463 red line is the fit of the linear model for the entire urban landscape at the STURLA pixel level.
464
465

References:

Albright, T. P., Pidgeon, A. M., Rittenhouse, C. D., Clayton, M. K., Flather, C. H., Culbert, P. D., & Radeloff, V. C. (2011). Heat waves measured with MODIS land surface temperature data predict changes in avian community structure. *Remote Sensing of Environment*. https://doi.org/10.1016/j.rse.2010.08.024

Azhdari, A., Soltani, A., & Alidadi, M. (2018). Urban morphology and landscape structure effect on land surface temperature: Evidence from Shiraz, a semi-arid city. *Sustainable Cities and Society*. https://doi.org/10.1016/j.scs.2018.06.034

Black, D., & Henderson, V. (1999). A theory of urban growth. *Journal of Political Economy*. https://doi.org/10.1086/250060

Bokaie, M., Zarkesh, M. K., Arasteh, P. D., & Hosseini, A. (2016). Assessment of Urban Heat Island based on the relationship between land surface temperature and Land Use/ Land Cover in Tehran. *Sustainable Cities and Society*. https://doi.org/10.1016/j.scs.2016.03.009

Buyantuyev, A., & Wu, J. (2010). Urban heat islands and landscape heterogeneity: Linking spatiotemporal variations in surface temperatures to land-cover and socioeconomic patterns. *Landscape Ecology*. https://doi.org/10.1007/s10980-009-9402-4

Chen, W., Xie, X., Wang, J., Pradhan, B., Hong, H., Bui, D. T., Duan, Z., & Ma, J. (2017). A comparative study of logistic model tree, random forest, and classification and regression tree models for spatial prediction of landslide susceptibility. *Catena*. https://doi.org/10.1016/j.catena.2016.11.032

Chen, X., & Zhang, Y. (2017). Impacts of urban surface characteristics on spatiotemporal pattern of land surface temperature in Kunming of China. *Sustainable Cities and Society*. https://doi.org/10.1016/j.scs.2017.03.013

Connors, J. P., Galletti, C. S., & Chow, W. T. L. (2013). Landscape configuration and urban heat island effects: Assessing the relationship between landscape characteristics and land surface temperature in Phoenix, Arizona. *Landscape Ecology*. https://doi.org/10.1007/s10980-012-9833-1

Cox, D. T. C., Hudson, H. L., Shanahan, D. F., Fuller, R. A., & Gaston, K. J. (2017). The rarity of direct experiences of nature in an urban population. *Landscape and Urban Planning*. https://doi.org/10.1016/j.landurbplan.2016.12.006

Cummings, L., Stewart, J. D., Kremer, P., & Shakya, K. (2021). *Associations between the Structure of Urban Landscape and Particulate Matter: A STURLA Case Study in Philadelphia, PA*. https://doi.org/10.20944/PREPRINTS202104.0588.V1

Danford, R. S., Strohbach, M. W., Warren, P. S., & Ryan, R. L. (2018). Active Greening or Rewilding the city: How does the intention behind small pockets of urban green affect use? *Urban Forestry and Urban Greening*. https://doi.org/10.1016/j.ufug.2017.11.014

DeSA, U. (2015). World population projected to reach 9.7 billion by 2050. *UN DESA United Nations Department of Economic and Social Affairs: New York, NY, USA*.

Fernández, J. E. (2007). Resource consumption of new urban construction in China. *Journal of Industrial Ecology*. https://doi.org/10.1162/jie.2007.1199

García, F. C., Bestion, E., Warfield, R., & Yvon-Durochera, G. (2018). Changes in temperature alter the relationship between biodiversity and ecosystem functioning. *Proceedings of the*

National Academy of Sciences of the United States of America. https://doi.org/10.1073/pnas.1805518115

Grimm, N. B., Faeth, S. H., Golubiewski, N. E., Redman, C. L., Wu, J., Bai, X., & Briggs, J. M. (2008). Global change and the ecology of cities. *Science*, *319*(5864), 756–760. https://doi.org/10.1126/science.1150195

Guhathakurta, S., & Gober, P. (2007). The impact of the Phoenix urban heat Island on residential water use. *Journal of the American Planning Association*. https://doi.org/10.1080/01944360708977980

Guo, A., Yang, J., Sun, W., Xiao, X., Xia Cecilia, J., Jin, C., & Li, X. (2020). Impact of urban morphology and landscape characteristics on spatiotemporal heterogeneity of land surface temperature. *Sustainable Cities and Society*. https://doi.org/10.1016/j.scs.2020.102443

Haase, D., Kabisch, S., Haase, A., Andersson, E., Banzhaf, E., Baró, F., Brenck, M., Fischer, L. K., Frantzeskaki, N., Kabisch, N., Krellenberg, K., Kremer, P., Kronenberg, J., Larondelle, N., Mathey, J., Pauleit, S., Ring, I., Rink, D., Schwarz, N., & Wolff, M. (2017). Greening cities – To be socially inclusive? About the alleged paradox of society and ecology in cities. *Habitat International*. https://doi.org/10.1016/j.habitatint.2017.04.005

Hackworth, J., & Smith, N. (2001). The changing state of gentrification. *Tijdschrift Voor Economische En Sociale Geografie*. https://doi.org/10.1111/1467-9663.00172

Hamstead, Z. A., Kremer, P., Larondelle, N., McPhearson, T., & Haase, D. (2016). Classification of the heterogeneous structure of urban landscapes (STURLA) as an indicator of landscape function applied to surface temperature in New York City. *Ecol. Indic.*, *70*, 574–585. https://doi.org/10.1016/j.ecolind.2015.10.014

Harris, C. D., & Ullman, E. L. (1945). The nature of cities. *The Annals of the American Academy of Political and Social Science*. https://doi.org/10.1177/000271624524200103

Hervé, M. (2020). *Package 'RVAideMemoire.'*

Howard, L. (2012). The Climate of London. In *The Climate of London*. https://doi.org/10.1017/cbo9781139226905

Huang, G., & Cadenasso, M. L. (2016). People, landscape, and urban heat island: dynamics among neighborhood social conditions, land cover and surface temperatures. *Landscape Ecology*. https://doi.org/10.1007/s10980-016-0437-z

Hudson Yards Development Corporation. (n.d.). *Hudson Yards*.

Jamei, Y., Rajagopalan, P., & Sun, Q. (Chayn). (2019). Spatial structure of surface urban heat island and its relationship with vegetation and built-up areas in Melbourne, Australia. *Science of the Total Environment*. https://doi.org/10.1016/j.scitotenv.2018.12.308

Jayalakshmy, M. S., & Philip, J. (2010). Thermophysical properties of plant leaves and their influence on the environment temperature. *International Journal of Thermophysics*. https://doi.org/10.1007/s10765-010-0877-7

Jenerette, G. D., Harlan, S. L., Brazel, A., Jones, N., Larsen, L., & Stefanov, W. L. (2007). Regional relationships between surface temperature, vegetation, and human settlement in a rapidly urbanizing ecosystem. *Landscape Ecology*. https://doi.org/10.1007/s10980-006-9032-z

Keniger, L. E., Gaston, K. J., Irvine, K. N., & Fuller, R. A. (2013). What are the benefits of interacting with nature? In *International Journal of Environmental Research and Public Health*. https://doi.org/10.3390/ijerph10030913

554 Kottmeier, C., Biegert, C., & Corsmeier, U. (2007). Effects of Urban Land Use on Surface
555 Temperature in Berlin: Case Study. *Journal of Urban Planning and Development*, *133*(2),
556 128–137. https://doi.org/10.1061/(asce)0733-9488(2007)133:2(128)
557 Kremer, P., Hamstead, Z. A., & McPhearson, T. (2013). A social-ecological assessment of vacant
558 lots in New York City. *Landscape and Urban Planning*.
559 https://doi.org/10.1016/j.landurbplan.2013.05.003
560 Kremer, P., Larondelle, N., Zhang, Y., Pasles, E., & Haase, D. (2018). Within-Class and
561 Neighborhood Effects on the Relationship between Composite Urban Classes and Surface
562 Temperature. *Sustainability*, *10*(3), 645. https://doi.org/10.3390/su10030645
563 Kuang, W., Liu, Y., Dou, Y., Chi, W., Chen, G., Gao, C., Yang, T., Liu, J., & Zhang, R. (2014). What
564 are hot and what are not in an urban landscape: quantifying and explaining the land
565 surface temperature pattern in Beijing, China. *Landscape Ecology*.
566 https://doi.org/10.1007/s10980-014-0128-6
567 Kuhn, M. (2008). caret Package. *Journal Of Statistical Software*.
568 Larondelle, N., Hamstead, Z. A., Kremer, P., Haase, D., & McPhearson, T. (2014). Applying a
569 novel urban structure classification to compare the relationships of urban structure and
570 surface temperature in Berlin and New York City. *Appl. Geogr.*, *53*, 427–437.
571 https://doi.org/10.1016/j.apgeog.2014.07.004
572 Lees. (2000). A reappraisal of gentrification: Towards a “geography of gentrification.” *Progress*
573 *in Human Geography*, *24*(3), 389–408. https://doi.org/10.1191/030913200701540483
574 Lees, L. (2003). Super-gentrification: The case of Brooklyn heights, New York City. *Urban*
575 *Studies*. https://doi.org/10.1080/0042098032000136174
576 Lu, Y., Nakicenovic, N., Visbeck, M., & Stevance, A. S. (2015). Policy: Five priorities for the un
577 Sustainable Development Goals. In *Nature*. https://doi.org/10.1038/520432a
578 McPhearson, T., Hamstead, Z. A., & Kremer, P. (2014). Urban ecosystem services for resilience
579 planning and management in New York City. *Ambio*, *43*(4), 502–515.
580 https://doi.org/10.1007/s13280-014-0509-8
581 Mills, J. G., Weinstein, P., Gellie, N. J. C., Weyrich, L. S., Lowe, A. J., & Breed, M. F. (2017). Urban
582 habitat restoration provides a human health benefit through microbiome rewilding: the
583 Microbiome Rewilding Hypothesis. *Restor. Ecol.*, *25*(6), 866–872.
584 https://onlinelibrary.wiley.com/doi/abs/10.1111/rec.12610?casa_token=hMKwkkcEjnYAA
585 AAA:EUkH6N_7thD2KBqWl9e3h5BRN-
586 rHGUoLG3QC5hL1FAWnk66u7v6E2pxqei83AsaHm7h-akXsmqeNh2XY
587 Mitz, E., Kremer, P., Larondelle, N., & Stewart, J. D. (2021). *Structure of Urban Landscape and*
588 *Surface Temperature : A Case Study in Philadelphia , PA*. *9*(March), 1–7.
589 https://doi.org/10.3389/fenvs.2021.592716
590 Molnár, V. (2017). New York’s New Edge: Contemporary Art, the High Line, and Urban
591 Megaprojects on the Far West Side. *Contemporary Sociology: A Journal of Reviews*.
592 https://doi.org/10.1177/0094306116681813cc
593 Morales, S. E., Biswas, A., Herndl, G. J., & Baltar, F. (2019). Global structuring of phylogenetic
594 and functional diversity of pelagic fungi by depth and temperature. *Frontiers in Marine*
595 *Science*. https://doi.org/10.3389/fmars.2019.00131
596 New York Downtown Alliance. (2013). *Back to Business: The State ofLower Manhattan Four*
597 *Months after HurricaneSandy*.

598 NYC Department of City Planning. (2021). *MapPluto Database*. New York State Government.
599 Oke, T. R. (1982). The energetic basis of the urban heat island. *Quarterly Journal of the Royal*
600 *Meteorological Society*. https://doi.org/10.1002/qj.49710845502
601 Oke, T. R. (1995). Classics in physical geography revisited: Sundborg, Å. 1951: Climatological
602 studies in Uppsala with special regard to the temperature conditions in the urban area.
603 Geographica 22. *Progress in Physical Geography*.
604 https://doi.org/10.1177/030913339501900105
605 Oliveira, S., Oehler, F., San-Miguel-Ayanz, J., Camia, A., & Pereira, J. M. C. (2012). Modeling
606 spatial patterns of fire occurrence in Mediterranean Europe using Multiple Regression and
607 Random Forest. *Forest Ecology and Management*.
608 https://doi.org/10.1016/j.foreco.2012.03.003
609 OS, B., & AA, A. (2016). Change Detection in Land Surface Temperature and Land Use Land
610 Cover over Lagos Metropolis, Nigeria. *Journal of Remote Sensing & GIS*, *5*(3), 1–8.
611 https://doi.org/10.4172/2469-4134.1000171
612 Patrick, D. J. (2014). The matter of displacement: a queer urban ecology of New York City's High
613 Line. *Social and Cultural Geography*. https://doi.org/10.1080/14649365.2013.851263
614 Ratti, C., Baker, N., & Steemers, K. (2005). Energy consumption and urban texture. *Energy and*
615 *Buildings*. https://doi.org/10.1016/j.enbuild.2004.10.010
616 Rook, G. A. (2013). Regulation of the immune system by biodiversity from the natural
617 environment: an ecosystem service essential to health. *Proc. Natl. Acad. Sci. U. S. A.*,
618 *110*(46), 18360–18367. https://doi.org/10.1073/pnas.1313731110
619 Sanchez, L., & Reames, T. G. (2019). Cooling Detroit: A socio-spatial analysis of equity in green
620 roofs as an urban heat island mitigation strategy. *Urban Forestry and Urban Greening*.
621 https://doi.org/10.1016/j.ufug.2019.04.014
622 Shanahan, D. F., Lin, B. B., Gaston, K. J., Bush, R., & Fuller, R. A. (2014). Socio-economic
623 inequalities in access to nature on public and private lands: A case study from Brisbane,
624 Australia. *Landscape and Urban Planning*.
625 https://doi.org/10.1016/j.landurbplan.2014.06.005
626 Soga, M., Yamaura, Y., Aikoh, T., Shoji, Y., Kubo, T., & Gaston, K. J. (2015). Reducing the
627 extinction of experience: Association between urban form and recreational use of public
628 greenspace. *Landscape and Urban Planning*.
629 https://doi.org/10.1016/j.landurbplan.2015.06.003
630 Stewart, J. D., Kremer, P., Shakya, K. M., Conway, M., & Saad, A. (2021). Outdoor Atmospheric
631 Microbial Diversity Is Associated With Urban Landscape Structure and Differs From Indoor-
632 Transit Systems as Revealed by Mobile Monitoring and Three-Dimensional Spatial Analysis
633 . In *Frontiers in Ecology and Evolution* (Vol. 9, p. 9).
634 https://www.frontiersin.org/article/10.3389/fevo.2021.620461
635 Susca, T., Gaffin, S. R., & Dell'Osso, G. R. (2011). Positive effects of vegetation: Urban heat
636 island and green roofs. *Environmental Pollution*.
637 https://doi.org/10.1016/j.envpol.2011.03.007
638 United States Census Burough. (2016). *New York City Census,*.
639 https://www.census.gov/quickfacts/newyorkcitynewyork
640 Voogt, J. A., & Oke, T. R. (1998). Effects of urban surface geometry on remotely-sensed surface
641 temperature. *International Journal of Remote Sensing*.

https://doi.org/10.1080/014311698215784
Walker, B., Holling, C. S., Carpenter, S. R., & Kinzig, A. (2004). Resilience, adaptability and transformability in social-ecological systems. *Ecology and Society*. https://doi.org/10.5751/ES-00650-090205
Weiss, N. (n.d.). *wPerm: Permutation tests. R package version 1.0. 1*.
Whitehand, J. W. R., Batty, M., & Longley, P. (1996). Fractal Cities: A Geometry of Form and Function. *The Geographical Journal*. https://doi.org/10.2307/3060277
Wolch, J. R., Byrne, J., & Newell, J. P. (2014). Urban green space, public health, and environmental justice: The challenge of making cities "just green enough." *Landscape and Urban Planning*. https://doi.org/10.1016/j.landurbplan.2014.01.017
Wong, M. S., Peng, F., Zou, B., Shi, W. Z., & Wilson, G. J. (2016). Spatially analyzing the inequity of the hong kong urban heat island by socio-demographic characteristics. *International Journal of Environmental Research and Public Health*. https://doi.org/10.3390/ijerph13030317
Zhou, W., Pickett, S. T. A., & Cadenasso, M. L. (2017). Shifting concepts of urban spatial heterogeneity and their implications for sustainability. *Landscape Ecology*, *32*(1), 15–30. https://doi.org/10.1007/s10980-016-0432-4